AMERICAN SOCIETY FOR MICROBIOLOGY | Journal of Virology

Recovery of West Nile Virus Envelope Protein Domain III Chimeras with Altered Antigenicity and Mouse Virulence

Alexander J. McAuley,[a,b] Maricela Torres,[a] Jessica A. Plante,[b,c*] Claire Y.-H. Huang,[d] Dennis A. Bente,[a,b,e,f] David W. C. Beasley[a,b,e,f]

Department of Microbiology & Immunology, University of Texas Medical Branch, Galveston, Texas, USA[a]; Institute for Human Infections and Immunity, University of Texas Medical Branch, Galveston, Texas, USA[b]; Department of Pathology, University of Texas Medical Branch, Galveston, Texas, USA[c]; Arbovirus Diseases Branch, Division of Vector-Borne Diseases, Centers for Disease Control and Prevention, U.S. Department of Health and Human Services, Fort Collins, Colorado, USA[d]; Center for Biodefense and Emerging Infectious Diseases, University of Texas Medical Branch, Galveston, Texas, USA[e]; Sealy Center for Vaccine Development, University of Texas Medical Branch, Galveston, Texas, USA[f]

ABSTRACT

Flaviviruses are positive-sense, single-stranded RNA viruses responsible for millions of human infections annually. The envelope (E) protein of flaviviruses comprises three structural domains, of which domain III (EIII) represents a discrete subunit. The EIII gene sequence typically encodes epitopes recognized by virus-specific, potently neutralizing antibodies, and EIII is believed to play a major role in receptor binding. In order to assess potential interactions between EIII and the remainder of the E protein and to assess the effects of EIII sequence substitutions on the antigenicity, growth, and virulence of a representative flavivirus, chimeric viruses were generated using the West Nile virus (WNV) infectious clone, into which EIIIs from nine flaviviruses with various levels of genetic diversity from WNV were substituted. Of the constructs tested, chimeras containing EIIIs from Koutango virus (KOUV), Japanese encephalitis virus (JEV), St. Louis encephalitis virus (SLEV), and Bagaza virus (BAGV) were successfully recovered. Characterization of the chimeras *in vitro* and *in vivo* revealed differences in growth and virulence between the viruses, with *in vivo* pathogenesis often not being correlated with *in vitro* growth. Taken together, the data demonstrate that substitutions of EIII can allow the generation of viable chimeric viruses with significantly altered antigenicity and virulence.

IMPORTANCE

The envelope (E) glycoprotein is the major protein present on the surface of flavivirus virions and is responsible for mediating virus binding and entry into target cells. Several viable West Nile virus (WNV) variants with chimeric E proteins in which the putative receptor-binding domain (EIII) sequences of other mosquito-borne flaviviruses were substituted in place of the WNV EIII were recovered, although the substitution of several more divergent EIII sequences was not tolerated. The differences in virulence and tissue tropism observed with the chimeric viruses indicate a significant role for this sequence in determining the pathogenesis of the virus within the mammalian host. Our studies demonstrate that these chimeras are viable and suggest that such recombinant viruses may be useful for investigation of domain-specific antibody responses and the more extensive definition of the contributions of EIII to the tropism and pathogenesis of WNV or other flaviviruses.

The *Flavivirus* genus is a large genus of viruses with positive-sense, single-stranded RNA genomes responsible for significant global morbidity and mortality (1). The fact that the majority are vector borne, being carried by either ticks or mosquitoes, allows them to have a wide geographical distribution and to be readily transmitted to humans. The clinical manifestations of flavivirus infections in humans vary considerably, with many causing nonspecific febrile illnesses that may progress to more severe syndromes, including hemorrhagic fever or encephalitis (1).

The surface of mature flavivirus virions is primarily comprised of 180 copies of the envelope (E) glycoprotein (2). As a result, the E protein is involved in the major steps of virus entry into susceptible cells, including the mediation of receptor binding and fusion between the viral envelope and host endosomal membranes, allowing the release of the viral genomic RNA into the cell cytoplasm for replication (3–6). These roles require considerable rearrangement of the E proteins on the surface of the mature virion, with important intra- and intermolecular interactions occurring at each stage (3, 7). Structurally, E may be divided into three major domains: EI, which in many West Nile virus (WNV) strains includes the single glycosylation motif; EII, which contains the fusion loop conserved among flaviviruses; and EIII, the putative receptor-binding domain (8). Although all three domains of the E protein appear to contribute to interactions with target cell ligands in different experimental systems, data that support a significant role for EIII in receptor binding come from investigations into competition between recombinant EIII molecules and infectious virions for adsorption to cell surfaces (9–11), immunological studies using neutralizing monoclonal antibodies (MAbs) targeting EIII (12), studies in which mutant viruses containing particular amino acid substitutions in EIII were generated (13–19), and investigations with dengue virus (DENV) E fusion pro-

Received 10 November 2015 **Accepted** 20 February 2016

Accepted manuscript posted online 24 February 2016

Citation McAuley AJ, Torres M, Plante JA, Huang CY-H, Bente DA, Beasley DWC. 2016. Recovery of West Nile virus envelope protein domain III chimeras with altered antigenicity and mouse virulence. J Virol 90:4757–4770. doi:10.1128/JVI.02861-15.

Editor: M. S. Diamond

Address correspondence to David W. C. Beasley, dwbeasle@utmb.edu.

* Present address: Jessica A. Plante, Gillings School of Global Public Health, University of North Carolina, Chapel Hill, North Carolina, USA.

teins (6). Studies of EIII protein subunits derived from different mosquito- and tick-borne flaviviruses have identified virus-specific differences in antigenicity, surface biochemistry, and structure, which further support a role for EIII as a key determinant of ligand binding and cell tropism for individual flavivirus types (20–28).

Construction of chimeric flaviviruses, whereby segments of the genome of one virus are substituted into the genome of a different flavivirus, has been used to investigate the roles of individual viral proteins in virulence or other phenotypes or to develop candidate vaccines and diagnostic reagents. In flaviviruses with chimeric structural proteins described previously, the coding sequences for complete structural proteins, usually prM and E, from a donor virus were substituted into a backbone virus (29–56). These chimeric viruses have antigenic characteristics that are determined by the donor structural proteins, and characterization of several has also identified significant shifts in *in vitro* growth and/or *in vivo* virulence phenotypes, consistent with the importance of the structural proteins and, in particular, E in those phenotypes. For example, the substitution of prM-E from tick-borne encephalitis virus (TBEV) into DENV serotype 4 (DENV-4) significantly affected the behavior of the virus both *in vitro* and *in vivo*, with growth in LLC-MK2 cells resulting in higher peak titers of the chimeric virus than the DENV-4 control and with intracerebral (i.c.) administration resulting in increased neurovirulence compared to the level of neurovirulence achieved with the equivalent dose of DENV-4 (30). Studies with similar chimeras comprised of prM-E from TBEV substituted into Omsk hemorrhagic fever virus (OHFV) as the backbone virus showed significantly earlier neuroinvasion by the chimeric virus than by the OHFV control, further indicating that the structural proteins can affect the behavior of the virus (52).

To date, few studies have attempted to generate chimeric proteins (i.e., proteins containing domains/regions derived from two or more different flaviviruses) and incorporate them into a viable virus. Given the discrete nature of EIII within the flavivirus E protein, as well as its role in receptor binding and as a target for virus-specific neutralizing antibodies, we hypothesized that substitution of EIII sequences between some flaviviruses would yield viable viruses but would likely be associated with significant changes in the growth, virulence, and/or antigenicity of the resulting chimeras. Therefore, the aims of this study were (i) to determine whether viable chimeras could be generated via the substitution of the EIII protein domain alone (i.e., chimerization of the E protein) and (ii) to assess the effects of EIII substitutions on the *in vitro* growth and *in vivo* pathogenesis of these chimeras. WNV, an encephalitic, mosquito-borne flavivirus, was used as the backbone virus for these initial investigations due to the availability of a well-characterized infectious clone system (57) and small-animal neuroinvasive disease models.

MATERIALS AND METHODS

WNV NY99 infectious clone and EIII donor viruses. For the generation of chimeric viruses, a previously described WNV infectious clone system was employed (57, 58). Briefly, the infectious clone consisted of two plasmids: pWN-AB, which contained the 5′ untranslated region (UTR) and the structural protein coding region, and pWN-CG, which contained the nonstructural protein coding region and the 3′ UTR. For virus recovery, the two plasmids were digested with XbaI and NgoMIV (New England BioLabs, Ipswich, MA) and ligated together after purification. The ligated full-length plasmid was linearized with XbaI, and full-length genome-equivalent RNA was produced by *in vitro* transcription from a T7 promoter upstream of the coding sequence using an Ampliscribe T7-Flash *in vitro* transcription kit (Epicentre Biotechnologies, Madison, WI). Virus recovery was carried out by electroporating the *in vitro*-transcribed RNA into Vero cells (ATCC, Manassas, VA) using an Invitrogen Neon transfection system (Life Technologies, Waltham, MA).

TABLE 1 EIII donor viruses used for chimerization

Donor virus[a]	Strain	Source
Koutango virus (KOUV)	Dak Ar D 5443	Viral RNA
Japanese encephalitis virus (JEV)	Nakayama	Viral RNA
St. Louis encephalitis virus (SLEV)	Parton	Viral RNA
Bagaza virus (BAGV)	DakAr B209	Viral RNA
Zika virus (ZIKV)	MR 766	Synthetic construct
Iguape virus (IGUV)	SPAn 71686	Viral RNA
Dengue 2 virus (DENV-2)	New Guinea C	Viral RNA
Yellow fever virus (YFV)	Asibi	Viral RNA
Powassan virus (POWV)/deer tick virus (DTV)	DTV IPS-001	Viral RNA

[a] EIII donor viruses were chosen on the basis of their genetic divergence from WNV NY99. Where possible, prototype donor viruses were used.

Four unique restriction sites (SalI at nucleotides [nt] 1829 to 1834, PstI at nt 1859 to 1864, StuI at nt 2183 to 2188, and BamHI at nt 2251 to 2256) were engineered into the pWN-AB plasmid by site-directed mutagenesis using QuikChange XL and Multi kits (Agilent Technologies, Santa Clara, CA). The locations of the sites were chosen on the basis of the strongly conserved amino acid sequences in these regions among many of the flaviviruses. Three of the four mutations were silent at the amino acid level; however, the mutation at the SalI site resulted in a conservative V290L amino acid substitution in E. This substitution has been identified in natural, pathogenic isolates of WNV, including the T2 strain from Turkey (59). Nine EIII donor viruses with increasing levels of genetic diversity from WNV were used (Table 1). cDNA for all but one of the viruses was derived from isolated viral RNA obtained from the World Reference Center for Emerging Viruses and Arboviruses (WRCEVA) at the University of Texas Medical Branch (UTMB). The Zika virus (ZIKV) EIII sequence was amplified from a synthetic construct purchased from Bio Basic Inc. (Markham, ON) on the basis of the published sequence with GenBank accession number NC_012532.

Construction of chimeric plasmids. Viral RNA was extracted from culture supernatant samples of each donor virus using the TRIzol reagent (Thermo Fisher Scientific, Waltham, MA), with RNA purification being performed using a Zymo Direct-Zol RNA purification kit (Zymo Research Corp., Irvine, CA). Reverse transcription to generate viral cDNA was performed using New England BioLabs avian myeloblastosis virus reverse transcriptase (New England BioLabs, Ipswich, MA). EIII inserts were amplified from cDNA generated from viral genomic RNA or a synthetic plasmid using the Roche High Fidelity PCR master mix (Roche, Indianapolis, IN). The PCR products were separated by agarose gel electrophoresis and purified using a Qiagen QIAquick gel extraction kit (Qiagen, Germantown, MD). Both the purified PCR products and backbone plasmids were digested with the appropriate restriction enzyme pairs (New England BioLabs, Ipswich, MA).

For seven of the EIII donor viruses, four chimera versions, denoted chimeric constructs A, B, C, and D, were generated using each combination of the up- and downstream restriction sites (Fig. 1A). For yellow fever virus (YFV) and deer tick virus (DTV), only the A- and B-form chimeric plasmids were generated. On the basis of the location of the restriction sites, the B form (PstI-StuI) had the smallest insert, consisting solely of EIII, whereas the A form (SalI-BamHI) had the largest substitution, containing part of EI upstream of the EI/EIII linker region and the first stem-helix region downstream. The C and D forms (with SalI-StuI and PstI-BamHI, respectively) had the additional upstream and downstream sequences, respectively. For the B forms, an infectious clone pWN-AB

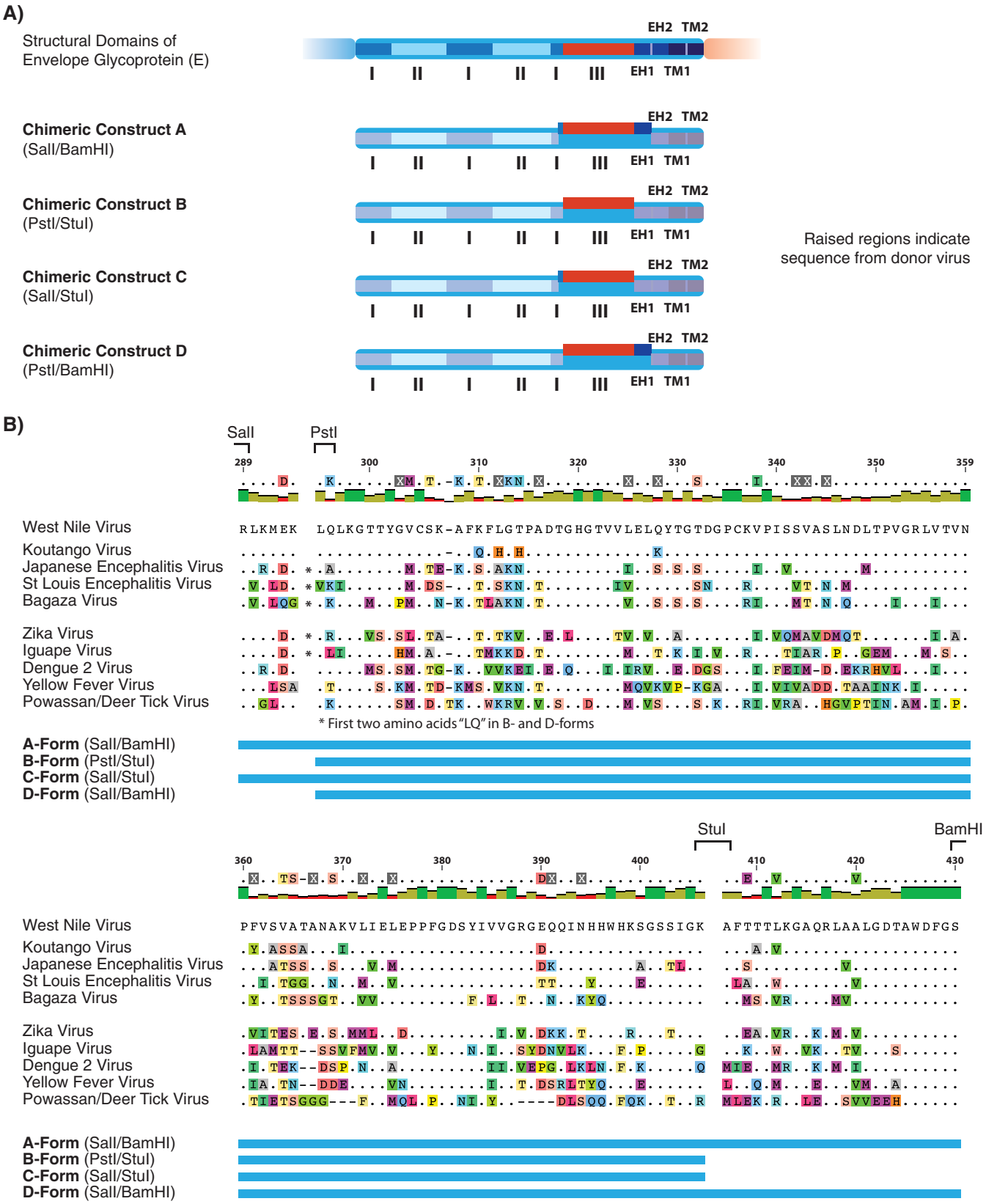

FIG 1 Schematic overview of chimera insert sizes and locations and sequence alignment of donor EIII sequences. (A) Donor EIII sequences were cloned into the WNV infectious clone using four combinations of up- and downstream restriction sites. The four resulting constructs were labeled A, B, C, and D. The A forms had the largest insertion size, with the donor virus EIII sequence being flanked by the donor virus EI sequence upstream and the first stem-helix structure downstream. The B forms contained donor virus EIII without the additional sequences, while the C and D forms contained the extra up- and downstream sequences, respectively. EH, E helical domain; TM, transmembrane domain. (B) Donor virus EIII amino acid sequences were aligned to determine the differences present in the chimeric viruses. Amino acid position numbers correspond to those of the WNV NY99 E sequence. Alignments were performed using the Geneious (v9.0.2) program (Biomatters, Auckland, New Zealand).

plasmid containing just PstI and StuI sites was used, thereby allowing chimeras without the SalI-associated V290L substitution to be generated.

The digested plasmids and inserts were gel purified and ligated overnight at 4°C using T4 DNA ligase (New England BioLabs, Ipswich, MA). The ligated plasmids were sequenced to confirm their identities and were transformed into *Escherichia coli* DH5α, from which glycerol stocks were generated for storage. Chimeric viruses were recovered following ligation of full-length genomic cDNA, *in vitro* transcription, and electroporation of the RNA into Vero cells as described above.

The construction of EIII chimeras using the WNV infectious clone was approved by the University of Texas Medical Branch Institutional Biosafety Committee. Only EIII sequences derived from viruses of the same or lower biosafety level (BSL) were used for attempts at chimerization, and all transfected cell cultures were handled under BSL-3 conditions. All subsequent experimentation with viable chimeric viruses occurred under BSL-3/animal BSL-3 (ABSL-3) conditions.

Nucleotide sequencing. Plasmids carrying the chimeric infectious clones and PCR-amplified viral cDNA generated from TRIzol-extracted RNA from the cell culture supernatant were submitted to the UTMB Molecular Genomics core facility for sequence determination using an Applied Biosystems 3130xl DNA sequencer (Applied Biosystems, Waltham, MA). The whole-genome sequences of recovered and serially passaged chimeric viruses were determined from purified viral RNA samples at the UTMB Next Generation Sequencing core facility using an Illumina HiSeq 1500 next generation sequencer (Illumina Inc., San Diego, CA).

Plaque, immunofocus, and TS assays. Virus titration was carried out in Vero cells grown in minimal essential medium (MEM; Corning, Manassas, VA) containing 8% fetal calf serum (FCS; HyClone, Logan, UT), 1× penicillin-streptomycin (Corning, Manassas, VA), 1× nonessential amino acids (Corning, Manassas, VA), and 1× L-glutamine (Life Technologies, Waltham, MA). Cells were plated in 6-well plates and grown until they reached approximately 90% confluence. Virus culture supernatant samples, serum samples, or homogenized organ tissue samples were serially 10-fold diluted (typical dilution range, 10^{-2} to 10^{-7}) in MEM containing 2% FCS. The diluted samples were transferred to the plated cells, and the viruses were allowed to incubate with the cells for 30 min at 37°C. After the incubation, the cells were overlaid with 4 ml per well of MEM-agar (1:1 ratio of 2% agar and 2× MEM [Quality Biological, Gaithersburg, MD] with 4% FCS and 2× supplements). The plates were incubated for 48 h at 37°C with 5% CO_2, after which 2 ml of MEM-agar containing 2% neutral red (Sigma-Aldrich, St. Louis, MO) was added to each well. The plates were incubated for a further 24 h before the plaques were counted. For crystal violet staining and immunostaining, the cells were fixed on day 3 postinfection with 10% buffered formalin (Fisher Scientific, Waltham, MA) before the agar plugs were removed. Cells were stained with crystal violet using a 0.25% crystal violet solution (Sigma-Aldrich, St. Louis, MO). Immunostaining was carried out by permeabilizing the cells using 70% ethanol per well, followed by incubation at −20°C for 30 min. The cells were blocked using phosphate-buffered saline containing 0.5% I-Block blocking reagent (Thermo Scientific, Pittsburgh, PA). The primary antibody used was an anti-WNV mouse immune ascitic fluid (MIAF; stock number T-35345) obtained from the WRCEVA. A horseradish peroxidase (HRP)-conjugated anti-mouse immunoglobulin secondary antibody (Sigma-Aldrich, St. Louis, MO) was used with True Blue HRP substrate (KPL, Gaithersburg, MD).

Temperature sensitivity (TS) has previously been used as a marker of the possible attenuation of virulence of naturally occurring and recombinant WNV variants (60–62), and TS assays were carried out as described above for the plaque assays. Duplicate plates were prepared for each sample, and following the first MEM-agar overlay, one of the plates was incubated at 37°C, while the other was incubated at 41°C. The plaque counts and morphologies at the two temperatures were compared following 72 h of total incubation, and a neutral red overlay was used to determine temperature sensitivity.

Virus stability. To compare the relative particle stability of the chimeric viruses, 1.2-ml 1:20 dilutions of each virus stock were prepared in MEM containing 2% FCS, with duplicate samples being placed at 37°C and 4°C. After thorough vortexing, 150 μl of each duplicate sample was harvested at the 0-h, 12-h, 24-h, 36-h, 48-h, and 72-h time points. The harvested samples were titrated in 12-well plates as described above for the plaque assays. The virus titers at each time point were determined and normalized to the values at 0 h to give a value of the percentage of virus remaining for each sample. The normalized data were plotted using GraphPad Prism (v6.0g) software (GraphPad, La Jolla, CA) and fitted with a one-phase decay nonlinear regression to determine particle half-lives with 95% confidence intervals (CIs).

Growth kinetics. Vero and C6/36 cells were plated in T-25 tissue culture flasks. Cells in triplicate flasks for each virus were infected with 1,000 PFU virus at a multiplicity of infection (MOI) of 5×10^{-4} to allow determination of minor differences in growth kinetics. The inoculating doses were confirmed by back-titration. Aliquots of supernatant of 500 μl were removed daily on days 0, 1, 2, 3, 4, and 5 postinfection and were clarified by centrifugation prior to storage at −80°C until titration. The virus titers in the samples were determined by plaque assay.

Western blotting. Cell lysates were prepared from the Vero cells used for the growth kinetics analysis on day 5 postinfection. Lysates were prepared using Invitrogen NuPAGE LDS sample buffer (Life Technologies, Waltham, MA) and were heat inactivated at 95°C for 30 min before being stored at −20°C until use. The nonreduced protein samples were run on 15-well NuPAGE Novex 4 to 12% bis-Tris protein gels (Life Technologies, Waltham, MA) using an XCell SureLock Mini-Cell gel tank (Life Technologies, Waltham, MA) in which the loading volume was normalized by the band intensity with the flavivirus EII-reactive 4G2 monoclonal antibody (EMD Millipore, Billerica, MA). Proteins were transferred to a nitrocellulose membrane (GE Healthcare Life Sciences, Pittsburgh, PA) using an XCell II blot module (Life Technologies, Waltham, MA). Following transfer, the blots were processed using a WesternBreeze chemiluminescent mouse kit (Life Technologies, Waltham, MA) following the manufacturer's instructions. Anti-WNV EIII-specific monoclonal antibody 3A3 (BioReliance Corp., Rockville, MD) and anti-JEV EIII monoclonal antibody ab81193 (Abcam, Cambridge, MA) were used to determine EIII antigenic specificity. MIAFs raised against WNV lineage I, WNV lineage II, Japanese encephalitis virus (JEV) Nakayama, St. Louis encephalitis virus (SLEV) Parton, and Bagaza virus (BAGV) DakAr B209 were acquired from the WRCEVA collection. Previously described human sera from WNV-infected patients were also used (63). The deidentified sera were used under an exemption approved by the UTMB Institutional Review Board. For the human sera, an HRP-conjugated anti-human IgG (Sigma-Aldrich, St. Louis, MO) was used with the Pierce SuperSignal West Femto reagent (Thermo Fisher, Waltham, MA). Antibody binding was detected via exposure of membranes to Amersham Hyperfilm ECL X-ray films (GE Healthcare Life Sciences, Pittsburgh, PA) that were developed using a Kodak X-OMAT 2000 X-ray film processor (Kodak, Rochester, NY).

Neutralization assays. Vero cells were plated in 12-well plates and grown until they were approximately 90% confluent. Once the cells were ready, serial 2-fold dilutions of MIAF and serum samples in MEM containing 2% FCS to a total volume of 60 μl per well were prepared in duplicate in 96-well plates. One well in each dilution series contained MEM–2% FCS only as a negative control. Previously titrated virus stocks were diluted to a final concentration of 1,000 PFU/ml, and 60 μl was added to each well, giving approximately 60 PFU per well. The virus-antibody mixtures were incubated at room temperature for an hour to allow neutralization to occur. After the incubation, 100 μl of the duplicate virus-antibody mixtures was added to each well on the 12-well plate, and each plate also contained duplicate wells with MEM and virus only as a control. The plates were incubated at room temperature for 30 min, before 2 ml of MEM-agar overlay was applied to each well. The plates were then incubated at 37°C with 5% CO_2 for 48 h, before being fixed with 10%

buffered formalin and immunostained as described above. Fifty percent neutralization titer (NT_{50}) values were determined for each virus-antibody combination by identifying the dilutions of antibody that led to a 50% reduction in focus number in the well compared to the focus number in the virus-only control wells.

Mouse virulence studies. Three- to 4-week-old female Swiss Webster mice (Harlan, Indianapolis, IN) were used as the animal model for WNV neuroinvasive disease, due to their susceptibility to infection with the WNV NY99 strain following inoculation via various routes (64, 65). All of the mice were housed in HEPA-filtered enclosures within the ABSL-3 facilities at UTMB and were provided with an unlimited supply of food and water. All animal studies were conducted in accordance with protocols approved by the UTMB IACUC.

The virulence of the viable chimeric viruses compared to that of WNV NY99 was determined following infection via the intraperitoneal (i.p.) or i.c. route of groups of 5 or 10 mice with 10 PFU (i.c.) and 100 PFU (i.p. and i.c.). The inocula were tested by back-titration to confirm the virus dose. Mice were checked daily for 21 days postinfection for signs of infection, with the checks increasing to twice daily once clinical signs started to develop.

Assessment of virus distributions in infected mice. Prior to infection, groups of five mice were anesthetized and subcutaneous IPTT-300 transponder microchips (BMDS, Seaford, DE) were injected to allow identification and temperature measurements. Temperature and weight data were recorded daily throughout the course of the experiment. On day 0, 5 mice that received microchips and an additional 15 mice that did not receive microchips were inoculated i.p. with 100 PFU of WNV NY99 or viable chimeric viruses. The virus titer in the inoculum was confirmed by back-titration. On days 1, 3, 5, 7, and 9 postinfection, groups of three mice that had not received microchips were selected at random from among the mice that had been inoculated with each virus and euthanized to collect blood via cardiac puncture and tissue samples. Blood samples were dispensed into EDTA-containing tubes (Sarstedt, Nümbrecht, Germany). Hematological analysis of the whole blood was carried out using a Hemavet 950 instrument (Drew Scientific, Miami Lakes, FL). Liver, spleen, kidney, lung, and brain tissue samples were removed and deposited in preweighed 2-ml homogenization tubes containing Lysing Matrix D (MP Biomedicals, Santa Ana, CA).

The anticoagulated blood samples were centrifuged at room temperature for 5 min at 10,000 × *g* to recover plasma, which was removed and stored at −80°C until needed. The organ tissue-containing tubes were weighed before and after addition of the tissue to determine tissue weights. Organ tissue weights were converted to volume equivalents (1 mg ≈ 1 μl), and MEM containing 2% FCS and 2× penicillin-streptomycin was added to each homogenization tube to reach a total volume of 500 μl. Samples were homogenized using a Qiagen TissueLyser II tissue disrupter (Qiagen, Germantown, MD) set to full speed for two 90-s cycles. The samples were spun down, and a further 500 μl of medium was added to each tube to achieve a total volume of 1 ml. The brain tissue samples were frozen at −80°C until needed, while the other organ tissue samples were further homogenized for two 120-s cycles at full speed. The samples were centrifuged again and stored at −80°C until needed. Virus titers in the plasma and organ tissue samples were determined by plaque assay starting at a 10^{-1} dilution, with titers being reported per milliliter of plasma and per 100 mg of tissue.

Statistical analyses. Statistical analysis of growth kinetics, plaque sizes, organ titer, and hematology data were performed by analysis of variance (ANOVA) with Bonferroni *post hoc* analysis using the Stata (v14) program (StataCorp, College Station, TX). Survival curve analysis was performed using a log-rank (Mantel-Cox) test with GraphPad Prism (v6.0g) software (GraphPad, La Jolla, CA). Comparison of average survival times was performed using a two-tailed Student's *t* test with Microsoft Excel software (Microsoft, Redmond, WA).

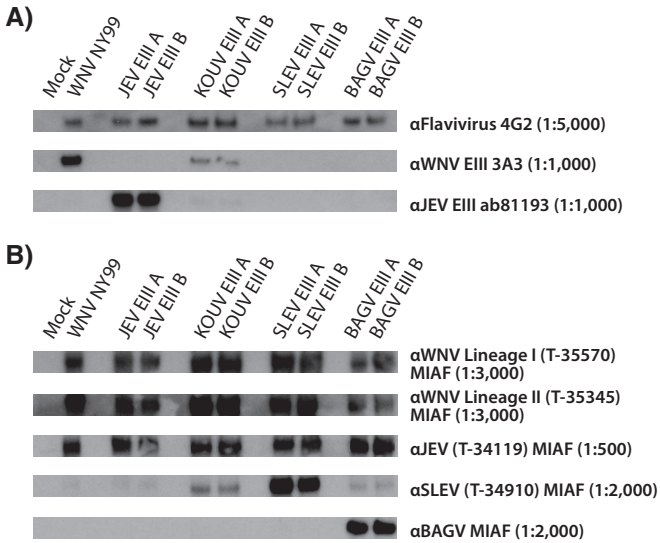

FIG 2 Antigenicity of chimeric viruses. (A) Reactivity of chimeric E proteins with monoclonal antibodies against flavivirus EII (MAb 4G2), WNV EIII (MAb 3A3), and JEV EIII (MAb ab81193); (B) reactivity of chimeric E proteins with various MIAFs.

RESULTS

Viability of chimeric viruses. Of the 30 EIII chimeras generated using the WNV infectious clone plasmids, 16 resulted in recoverable viruses: all four versions of the four donor viruses most similar to WNV (Koutango virus [KOUV], JEV, SLEV, and BAGV). Deep sequencing of the viable viruses recovered at passage 0 (P0) revealed only one nonsynonymous mutation present at a frequency of over 20%: an N222Y substitution present at a >80% frequency in each of the SLEV C/D and BAGV B/C chimeras. Cells transfected with the nonviable chimeric constructs failed to release infectious particles into the supernatant following electroporation (as determined by reverse transcription-PCR). Immunostaining of the electroporated cell monolayers revealed staining of individual cells when an anti-WNV MIAF was used but not when the anti-flavivirus EII MAb 4G2 was used (data not shown), suggesting that E-protein folding was impaired.

Antigenicity of chimeric viruses. Western blotting assays performed using whole-cell lysates prepared from Vero cells infected with the A or B forms of the chimeras, as well as WNV NY99, showed similar reactivities with the anti-flavivirus EII 4G2 MAb (Fig. 2A). The anti-WNV EIII MAb 3A3 had slightly reduced reactivity with the KOUV chimeras and was not reactive with any of the other chimeras. The anti-JEV EIII MAb (ab81193) was reactive with the JEV EIII A/B chimeras only. Specific antibodies against the EIIIs of the other donor viruses were not available, so instead, MIAFs raised against the donor viruses were used to compare antigenicity changes associated with EIII substitutions (Fig. 2B). Two anti-WNV MIAFs, one against a lineage I WNV strain and another against a lineage II WNV strain, showed strong binding with all the chimeras, most likely due to antibodies targeting epitopes in domains I and II of the E protein that were retained in the chimeras. The JEV MIAF also showed significant cross-reactivity, with the band intensities for the JEV chimeras being similar to those for the other viruses, consistent with the closer antigenic relatedness of WNV and JEV. The SLEV and BAGV MIAFs

A)

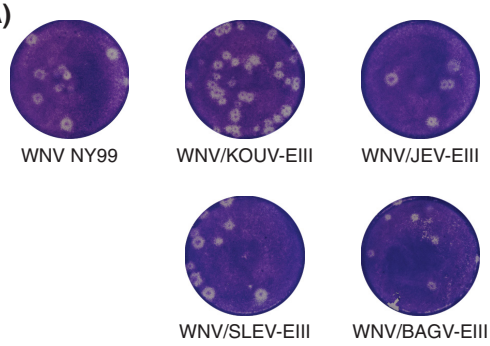

B)

Virus	Plaque Size	Std Dev
WNV/KOUV-EIII	**2.30mm**	0.42mm
WNV/JEV-EIII	3.15mm	0.47mm
WNV/SLEV-EIII	3.30mm	0.71mm
WNV/BAGV-EIII	**1.95mm**	0.37mm
WNV NY99	3.60mm	0.52mm

C)

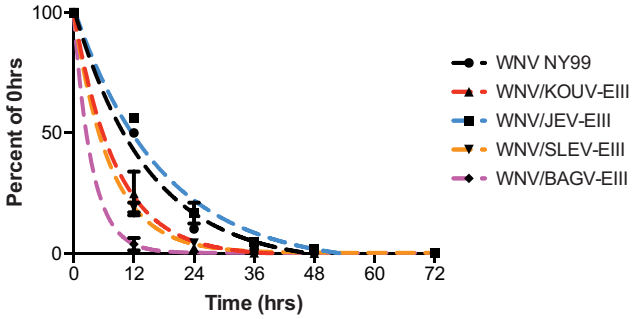

FIG 3 Plaque morphology and particle stability of chimeric viruses. (A) After 72 h of incubation, the plaque morphologies of WNV/KOUV-EIII and WNV/BAGV-EIII in Vero cells were significantly smaller than those of WNV NY99, whereas those of WNV/JEV-EIII and WNV/SLEV-EIII remained similar to those of the NY99 control. (B) Ten representative plaques were measured for each chimera, with the mean and standard deviation (Std Dev) plaque sizes being determined for each. Plaque sizes statistically significantly different from those of WNV NY99 ($P < 0.05$, as determined by one-way ANOVA with the Bonferroni correction) are in bold. (C) Duplicate virus (WNV NY99 and EIII chimeras) samples were held at 37°C, and aliquots were harvested at 0, 12, 24, 36, 48, and 72 h. Samples were titrated, and the values were normalized to the titer at 0 h. One-phase decay curves were fitted to the data using GraphPad Prism (v6.0g) software.

showed much less cross-reactivity. The BAGV MIAF reacted only with the BAGV chimeras, in agreement with its grouping in the Ntaya rather than the JE serocomplex.

Due to the higher recovery titers, the greater apparent tolerance of the B-form EIII substitutions, and the lack of distinct antigenic differences between the A and B forms, the B forms were utilized for further comparative characterization and are henceforth referred to as WNV/JEV-EIII, WNV/KOUV-EIII, WNV/SLEV-EIII, and WNV/BAGV-EIII.

Plaque morphology of recovered chimeric viruses. Distinct and statistically significant differences in plaque sizes were observed between WNV NY99 and some of the chimeras (Fig. 3A and B). Ten representative plaques were measured for each virus, and the sizes were compared by one-way ANOVA with the Bonferroni correction. For WNV NY99, the plaques in Vero cells after 72 h were large and distinct (3.60 ± 0.52 mm). WNV/JEV-EIII had a mean plaque size 0.45 mm smaller than that of WNV NY99 (3.15 ± 0.47 mm), although this difference was not statistically significant ($P > 0.05$). In contrast, WNV/KOUV-EIII had a significantly smaller plaque size than WNV NY99 (2.30 ± 0.42 mm; $P < 0.001$), with the mean diameter of 1.3 mm for WNV/KOUV-EIII plaques being smaller than that for NY99 plaques. Similarly, WNV/BAGV-EIII had a significantly smaller plaque size than WNV NY99 (1.95 ± 0.37 mm; $P < 0.001$), with the mean diameter of the plaques being 1.65 mm smaller than that of NY99 plaques. WNV/SLEV-EIII generated large plaques (3.30 ± 0.71 mm) whose sizes were not significantly different from those of WNV NY99 plaques.

Stability and TS of chimeric viruses. WNV NY99 and all four chimeras demonstrated high degrees of stability at 4°C, with less than a 2-fold decrease in titer being noted after 72 h (data not shown). Some variability between the chimeras was observed when they were held at 37°C (Fig. 3C). WNV NY99 was calculated to have a half-life of 10.31 h (95% CI, 8.26 to 13.71 h), while WNV/JEV-EIII had a half-life of 12.13 h (95% CI, 9.58 to 16.53 h). Both WNV/KOUV-EIII and WNV/SLEV-EIII had half-lives approximately 2-fold shorter than the half-life of NY99 (5.88 h [95% CI, 4.74 to 7.75 h] and 5.02 h [95% CI, 4.75 to 5.32 h], respectively). The chimera with the most divergent EIII sequence, WNV/BAGV-EIII, had a half-life 4-fold shorter than that of NY99 (2.51 h [95% CI, 2.12 to 3.09 h]).

Previous studies have used temperature sensitivity (TS) assays (comparison of the virus titer and plaque morphology at 37°C and 41°C) as a marker of the possible attenuation of the virulence of WNV strains (60–62). Accordingly, TS assays were run with WNV NY99 and the EIII chimeras (Table 2). No significant differences in the titers of any of the viruses titrated at the two temperatures were observed; however, the plaque size of WNV/BAGV-EIII was significantly smaller at 41°C than at 37°C (diameter, <0.5 mm versus 2.0 mm).

Growth kinetics of chimeric viruses in Vero and C6/36 cells. WNV NY99 and the four chimeras were grown in Vero and C6/36 cells following infection at a low MOI of 0.0005 to determine growth kinetics (Fig. 4). WNV/JEV-EIII grew very similarly to WNV NY99 in both cell types, with no significant differences in titer being detected at any of the time points at which titers were measured. In Vero cells, the growth of WNV/KOUV-EIII was similar to that of WNV/SLEV-EIII for the first 2 days, with the titers on these days being within 5-fold of those of WNV NY99. From

TABLE 2 TS of WNV EIII chimeras

Virus	Titer at:		Log_{10} difference in titer	*P* value[a]
	37°C	41°C		
WNV NY99	3.73×10^8	3.85×10^8	−0.013	0.418
WNV/KOUV-EIII	2.27×10^8	1.78×10^8	0.104	0.109
WNV/JEV-EIII	3.21×10^8	2.45×10^8	0.118	0.146
WNV/SLEV-EIII	3.70×10^7	1.45×10^7	0.406	0.135
WNV/BAGV-EIII	3.80×10^6	2.30×10^{6b}	0.218	0.081

[a] Titers were compared by one-way ANOVA with the Bonferroni correction.
[b] The average plaque size was significantly smaller (<0.5 mm) at 41°C than at 37°C (2.0 mm).

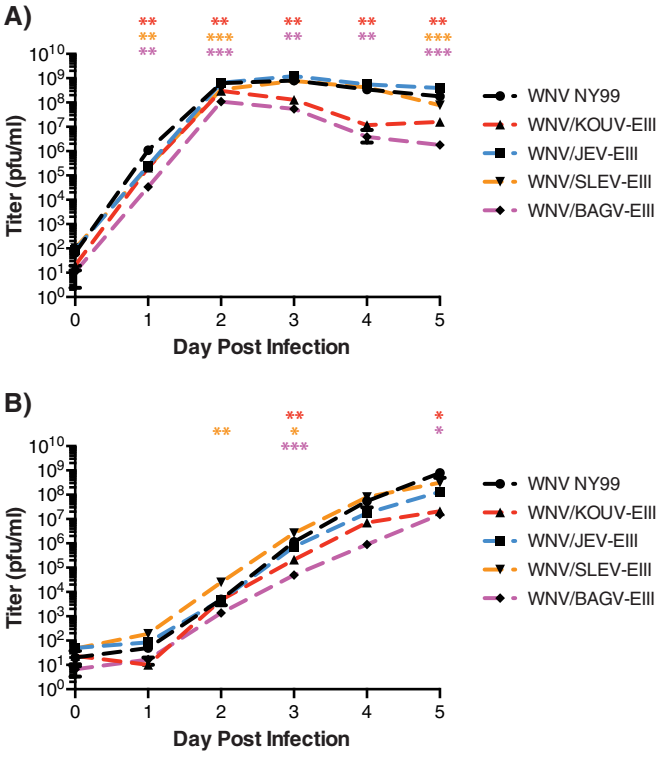

FIG 4 *In vitro* growth kinetics for chimeric viruses. Growth kinetics were determined for WNV NY99 and each of the four chimeras following infection of Vero (A) and C6/36 (B) cells in triplicate flasks at a low MOI of 0.0005. Statistical significance was determined by ANOVA with the Bonferroni correction for all viruses by comparison to the results for WNV NY99 (*, $P < 0.05$; **, $P < 0.01$; ***, $P < 0.001$; the different colors correspond to individual chimeras). The graphs show mean values with standard errors.

day 3 onward, the titers of WNV/KOUV-EIII declined more rapidly than those of WNV NY99, although the titers of WNV/SLEV-EIII remained similar to those of WNV NY99 from days 3 to 5, with no significant differences being noted on either day 3 or 4. Within C6/36 cells, WNV/KOUV-EIII grew similarly to WNV NY99, although the titers of WNV/KOUV-EIII were significantly lower than those of NY99 on days 3 and 5. In contrast, in C6/36 cells, WNV/SLEV-EIII grew with titers significantly higher than those of WNV NY99 on days 2 and 3, but the titers on days 4 and 5 were within 2-fold of those of NY99.

WNV/BAGV-EIII displayed the most significant difference in growth from that of WNV NY99 in both cell types. Within Vero cells, the initial growth of WNV/BAGV-EIII was slower than that of NY99, and WNV/BAGV-EIII had a statistically significant 33-fold lower titer than NY99 on day 1. However, by day 2 the WNV/BAGV-EIII titer had increased so that it was only 5-fold lower than that of WNV NY99. Similar to the findings for WNV/KOUV-EIII, the titers of WNV/BAGV-EIII declined more rapidly than those of WNV NY99 on days 3 to 5. In C6/36 cells, the growth of WNV/BAGV-EIII was retarded, with titers significantly lower than those of NY99 being detected on day 3 and day 5 (12-fold and 51-fold lower, respectively).

Sequence stability of chimeric viruses. All four of the chimeric viruses, as well as WNV NY99, were passaged 10 times in Vero cells, and the E-coding region was sequenced to determine sequence stability in and around the EIII region. At P10, WNV NY99 had a single amino acid substitution in E, E390G, a previously described tissue culture adaptation that affects glycosaminoglycan binding (15, 16). No mutations were detected in either the WNV/JEV-EIII or WNV/KOUV-EIII E sequence at P10. Both the WNV/SLEV-EIII and WNV/BAGV-EIII P10 chimeras encoded a consensus N222Y substitution, with WNV/BAGV-EIII also possessing a conservative L311I mutation at P10.

Neutralization of chimeric viruses. Neutralization of the chimeric viruses with anti-WNV MIAFs, a rabbit serum raised against WNV EIII (63), and two serum samples obtained from WNV-infected humans (63) demonstrated antigenic differences among the different chimeras, particularly with WNV/JEV-EIII (Table 3). As expected, rabbit anti-WNV EIII polyclonal serum showed the greatest WNV-specific activity, with strong neutralization of WNV NY99 and WNV/KOUV-EIII but a significantly weaker neutralization of all of the other chimeras. Significant differences in neutralizing activity against the EIII chimera viruses were also observed for both of the anti-WNV MIAFs. The anti-WNV lineage I MIAF neutralized the WNV/KOUV-EIII and WNV/BAGV-EIII chimeras to levels similar to those at which it neutralized WNV NY99 (NT_{50}s, 2,560 to 5,120), but WNV/JEV-EIII and WNV/SLEV-EIII were significantly less well neutralized (NT_{50}s, 640). Similar results were also seen with the anti-WNV lineage II MIAF, although the WNV/BAGV-EIII chimera was less readily neutralized by the lineage II MIAF than by the lineage I MIAF. Consistent with previous reports that relatively little of the neutralizing antibody response in humans targets epitopes in EIII, both human serum samples neutralized all chimeras to levels comparable to those at which they neutralized the NY99 parent, with the exception of an 8-fold lower neutralization titer for WNV/JEV-EIII with the 026 human serum sample than the 022 human serum sample. A >4-fold change in neutralization titer compared to that of WNV NY99 was deemed significant.

TABLE 3 Neutralization of WNV EIII chimeras by polyclonal antisera

Virus	$PRNT_{50}$[a]				
	Anti-WNV EIII rabbit pAb[b]	Lineage I MIAF (T-35570)	Lineage II MIAF (T-35345)	Anti-WNV human serum 022	Anti-WNV human serum 026
WNV NY99	1,280	5,120	1,280	1,280	10,240
WNV/KOUV-EIII	2,560	2,560	2,560	1,280	10,240
WNV/JEV-EIII	80	640	80	1,280	1,280
WNV/SLEV-EIII	<40	640	80	1,280	5,120
WNV/BAGV-EIII	<40	2,560	640	1,280	5,120

[a] $PRNT_{50}$, 50% plaque reduction neutralization titer.
[b] pAb, polyclonal antibody.

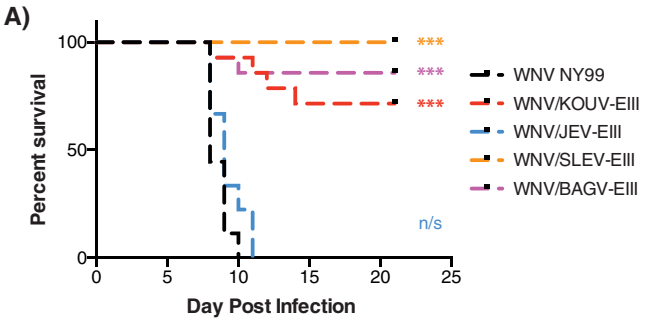

Virus	AST (Days)	Std Dev
WNV NY99	8.56	0.73
WNV/KOUV-EIII	**11.25**	2.5
WNV/JEV-EIII	9.22	1.20
WNV/SLEV-EIII	N/A	
WNV/BAGV-EIII	9.00	1.41

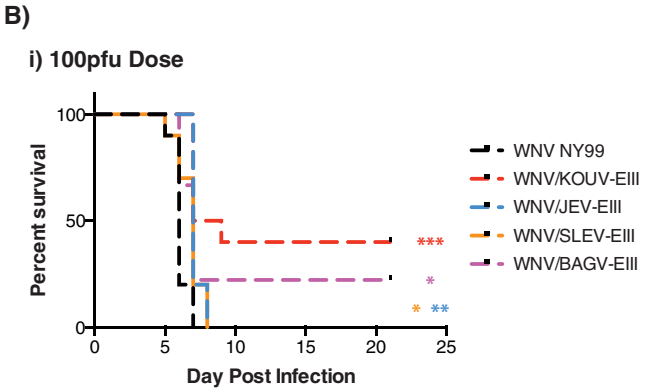

Virus	AST (Days)	Std Dev
WNV NY99	6.10	0.57
WNV/KOUV-EIII	**7.33**	0.82
WNV/JEV-EIII	**7.20**	0.45
WNV/SLEV-EIII	6.80	0.92
WNV/BAGV-EIII	6.57	0.53

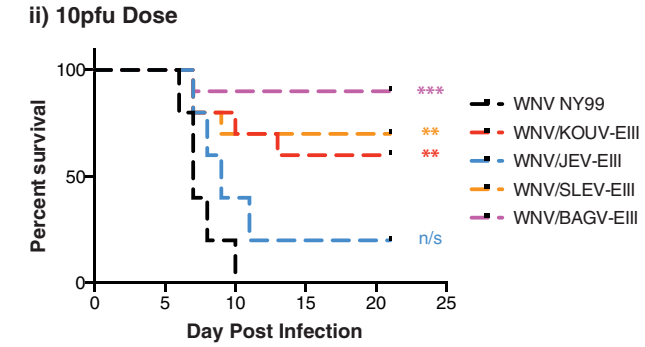

Virus	AST (Days)	Std Dev
WNV NY99	6.70	1.52
WNV/KOUV-EIII	9.25	2.87
WNV/JEV-EIII	8.75	1.71
WNV/SLEV-EIII	7.67	1.15
WNV/BAGV-EIII	7.00	N/A

FIG 5 Virulence of chimeric viruses following i.p. and i.c. inoculation. (A) Three- to 4 week-old female Swiss Webster mice were infected with 100 PFU of virus i.p. ($n = 10$ or 14). (B) Swiss Webster mice were infected with WNV NY99 ($n = 5$ per group) or an EIII chimera ($n = 5$ per group for WNV/JEV-EIII, $n = 10$ per group for WNV/KOUV-EIII, WNV/SLEV-EIII, and WNV/BAGV-EIII) at 100 or 10 PFU via the i.c. route. For the mice that succumbed to infection, average survival times (ASTs) with standard deviations were calculated and are shown on the right. Comparison of the mortality curves for mice infected with the chimeric viruses and those for mice infected with WNV NY99 for statistically significant differences was performed using a log-rank (Mantel-Cox) test (*, $P < 0.05$; **, $P < 0.01$; ***, $P < 0.001$). Comparison of the average survival times of mice infected with the chimeric viruses and those of mice infected with WNV NY99 for statistically significant differences was performed using a two-tailed Student's *t* test, with statistically significant differences being indicated in bold ($P < 0.05$).

Mouse virulence studies. In order to determine the effects of chimerization on virulence following peripheral infection, groups of 10 or 14 3- to 4-week-old female Swiss Webster mice were inoculated via the i.p. route with 100 PFU of WNV NY99 or a chimeric virus (Fig. 5A). WNV/JEV-EIII maintained high virulence, with no significant differences in survival between mice infected with WNV/JEV-EIII and mice infected with WNV NY99 being detected. WNV/KOUV-EIII caused significantly lower mortality (25%) than the NY99 parent virus or the JEV chimera, and mice infected with WNV/KOUV-EIII displayed protracted survival times compared with the average survival times of mice infected with WNV NY99 and the other chimeras. Surprisingly, the virulence of WNV/SLEV-EIII was completely attenuated following i.p. inoculation, despite efficient growth *in vitro*. Interestingly, even though WNV/BAGV-EIII had the most distinct EIII sequence of the donor viruses, it caused 14% mortality. Viruses isolated from mouse brains following lethal KOUV and BAGV chimera infections had no additional mutations in E, suggesting that further adaptation of the chimeric E sequence was not required for neuroinvasion leading to lethal disease in those animals.

Owing to the significant differences in neuroinvasive disease following i.p. inoculation, the neurovirulence of the chimeras was assessed by direct intracranial inoculation (Fig. 5B). Groups of 5 or 10 mice were infected with 10 or 100 PFU of WNV NY99 or a chimeric virus via the i.c. route. As expected, WNV NY99 (which

has a 50% lethal dose of <1 PFU when given i.c.) was universally lethal at both challenge doses. Similar to the results obtained with the i.p. inoculations, WNV/JEV-EIII caused high rates of mortality at both doses, although one of the five animals survived following infection with the 10-PFU dose. At the 10-PFU dose, WNV/SLEV-EIII, WNV/KOUV-EIII, and WNV/BAGV-EIII all appeared to have lower neurovirulence than WNV NY99, with the mortality rates for mice infected with these three chimeras being reduced compared to those for mice infected with WNV NY99. At the 100-PFU dose, the mortality rates for mice infected with WNV/KOUV-EIII and WNV/BAGV-EIII were 60% and 80%, respectively.

Assessment of virus distributions in infected mice. Peripheral inoculation with 100 PFU of each virus had revealed that the virulence of some of the EIII chimeras was significantly attenuated compared to that of WNV NY99, despite similar *in vitro* growth, plaquing, temperature sensitivity, and particle stability phenotypes. In order to better characterize the course of infection, a serial sacrifice study was carried out with mice infected with one of the four chimeras and WNV NY99. Cohorts of 20 mice were dosed with 100 PFU of each virus via the i.p. route, with the inoculating doses being confirmed by back-titration. Microchips were placed in 5 mice in each cohort to allow daily temperature and weight measurements, and for each virus, an additional 15 mice that did not receive microchips were used for biosampling on days 1, 3, 5, 7, and 9.

The temperatures of all of the mice remained similar for the first 7 days of the infection. For the WNV NY99- and WNV/JEV-EIII-infected mice, rapid declines in body temperature (approximately 3°C per day) were observed from day 8 until death (Fig. 6A). Similarly, the lethal KOUV B-form infections also resulted in body temperature reductions, although these were less rapid, with the rate of temperature loss rarely exceeding 1°C per day. Temperature changes were not observed during nonlethal infections or in mice that died prior to day 9. Weight loss was observed with all of the infected mice starting on day 7. Three weight loss profiles were identified (Fig. 6B): a rapid loss of up to 3 g between day 7 and the time of death or euthanasia following infection with WNV NY99 and WNV/JEV-EIII, an approximately 2-g weight loss between days 7 and 14 following infection with WNV/KOUV-EIII and WNV/SLEV-EIII, and a small, 2-day decrease following infection with WNV/BAGV-EIII.

All of the viruses generated detectable viremia that peaked on day 3 postinfection (Fig. 7A). For WNV NY99 and WNV/KOUV-EIII, viremia was mostly detectable only on days 1 and 3, with the mean peak titers for both viruses being very similar at approximately 10^5 PFU/ml. WNV/JEV-EIII also generated a robust viremia, although the peak viremia of WNV/JEV-EIII was almost 7-fold lower than that of WNV NY99. Moreover, the duration was protracted compared to that for NY99, with the majority of the mice still having detectable viremia on day 5. Both WNV/SLEV-EIII and WNV/BAGV-EIII generated viremias in only a subset of animals at each time point during days 3 to 7, and the peak viremias were considerably lower than those of the other viruses.

As expected, neuroinvasion was consistently seen with WNV NY99 (Fig. 7B) beginning on day 5. Curiously, despite causing 100% mortality, neuroinvasion with WNV/JEV-EIII was less consistent, with at least one virus-negative brain sample being detected at each of the later time points. In spite of the lack of mortality associated with the WNV/SLEV-EIII chimera,

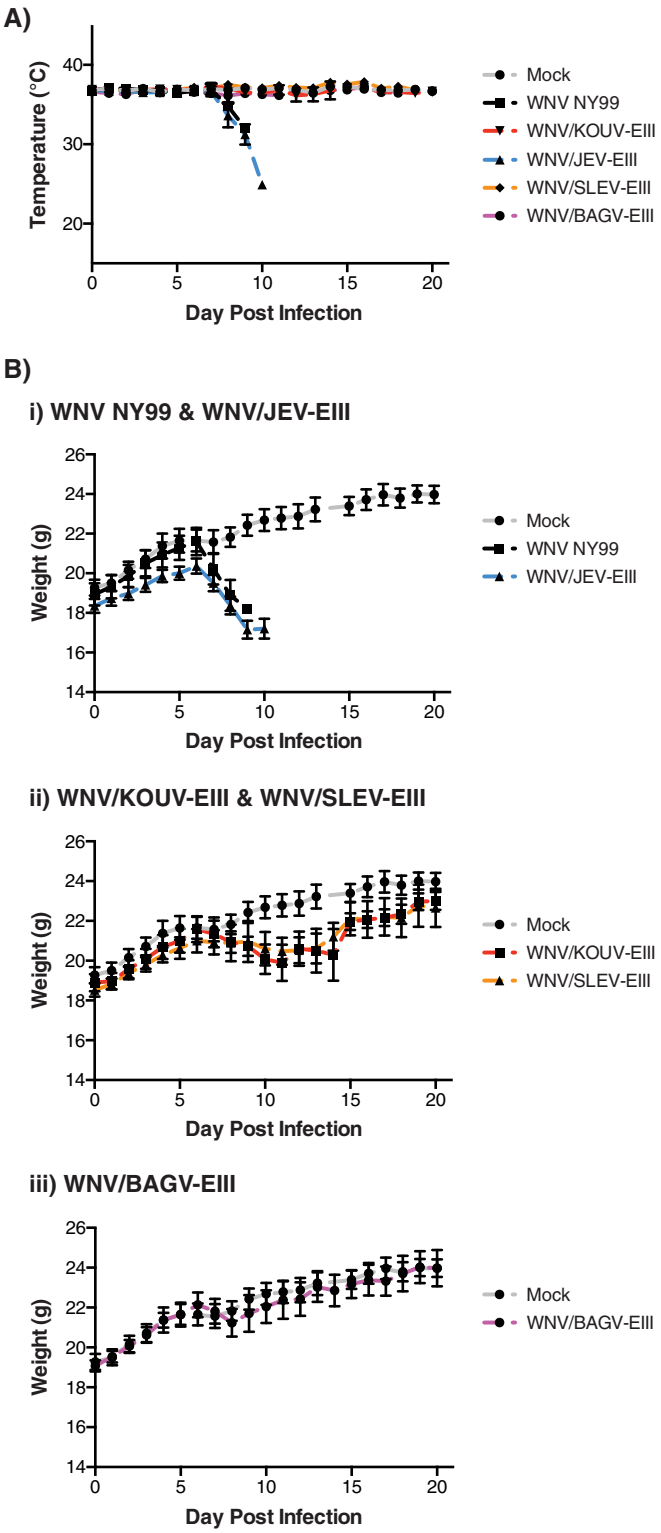

FIG 6 Temperature and weight changes following i.p. inoculation with EIII chimeras. Groups of five 3- to 4-week-old female Swiss Webster mice were infected with 100 PFU of WNV NY99 or an EIII chimera via the i.p. route. Temperatures (A) and weights (B) were measured daily for 21 days following infection. Three different weight profiles emerged: one for the WNV NY99- and WNV/JEV-EIII-infected mice (Bi), a second one for the WNV/KOUV-EIII- and WNV/SLEV-EIII-infected mice (Bii), and a third for the WNV/BAGV-EIII-infected mice (Biii).

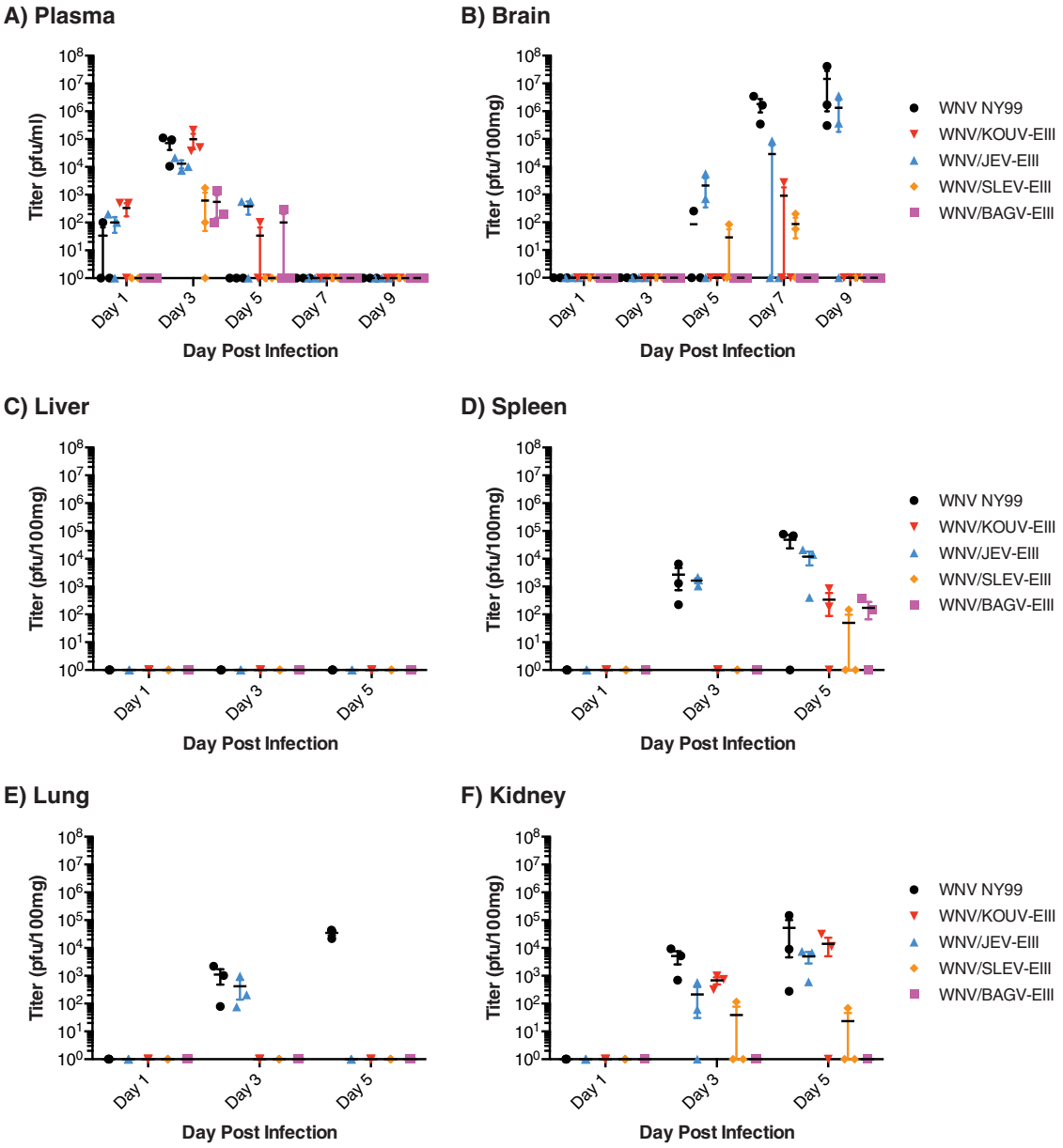

FIG 7 Organ titers following i.p. inoculation. Three- to 4-week-old female Swiss Webster mice were inoculated with either WNV NY99 or an EIII chimera at 100 PFU i.p. Three mice per group were euthanized on days 1, 3, 5, 7, and 9, and blood and organs were removed for titration. Plasma (A) and brain (B) titers were determined at all time points, while liver (C), spleen (D), lung (E), and kidney (F) titers were determined on days 1, 3, and 5. The graphs show individual values with means and standard errors.

occasional neuroinvasion was detected on days 5 and 7 (i.e., after the detection of viremia) but was not associated with any clinical signs of infection. Despite the occasional mortality observed during the initial comparisons with WNV/KOUV-EIII- and WNV/BAGV-EIII-infected mice, only one WNV/KOUV-EIII-infected mouse had detectable neuroinvasion in this experiment.

Titers in the peripheral organs were also variable between the viruses (Fig. 7C to F). WNV NY99 consistently grew to high titers in all of the organs studied, except the liver. WNV/JEV-EIII had a distribution similar to that of WNV NY99, but the titers were generally lower than those of NY99, and in contrast to NY99, the virus appeared to be more readily cleared from the lung. Despite the strong, WNV NY99-like viremia generated by the WNV/KOUV-EIII chimera, it was rarely detected in peripheral organs with the exception of the kidney, in which it grew similarly to the parental virus, suggesting a potential shift in tissue tropism for that chimera. WNV/SLEV-EIII and WNV/BAGV-EIII were infrequently detected in peripheral organs, with even the kidney only occasionally having detectable titers.

Hematological analysis at each time point revealed few differences of note (data not shown). There were no significant differences in the total white blood cell count between the infected and mock-infected mice, although the data suggested a trend toward

leukocytopenia in all infected mice, particularly early in the infection, mostly resulting from apparent lymphocytopenia. Alterations to red blood cell counts and their associated metrics were minimal.

DISCUSSION

The envelope glycoprotein is the main protein component present on the surface of mature flavivirus virions and is responsible for a range of processes during viral attachment and entry. Previous studies have suggested that EIII contributes significantly to the binding of flaviviruses to cell surface receptors (6, 10, 12, 28, 66, 67), although other regions of the E protein also contribute to interactions with cell surface ligands. A previous study by Bielefeldt-Ohmann et al. showed that truncated, secretable chimeric E proteins incorporating the EIII domain from DENV-3 and the EI-EII domains from DENV-2 could be expressed from mammalian cells and maintained the antigenic properties of both protein regions (68), while a recent paper by Gallichotte et al. has demonstrated that viruses with interserotype substitutions of EIII (DENV-4 with DENV-2 EIII) are viable and that such substitutions lead to the generation of chimeras with shared antigenic properties (69).

We aimed to test the tolerance of WNV for substituted EIII sequences and the effects that such substitutions may have on the growth, virulence, and antigenicity of the chimeric viruses. Our data clearly show that EIII substitution is feasible for the generation of infectious chimeric WNVs but that there are substantial constraints on the sequence identity of the substituted domain: recoverable viruses had amino acid identities greater than 65% in both EIII and E as a whole compared to the sequence of WNV NY99, while more divergent EIII sequences were not tolerated. Analysis of the sequences that were tolerated and not tolerated did not reveal any obvious shared motifs or structural features that allowed chimera viability (Fig. 1B), but it seems likely that the constraints on EIII substitution are imposed by intra- and intermolecular interactions between EIII and the rest of E as well as, potentially, between EIII and prM/M.

As expected, substitution of alternative EIII sequences led to antigenic changes in the chimeric proteins that were detectable by Western blotting using virus-specific MAbs or polyclonal MIAFs. Previous studies by others have demonstrated that depletion of anti-EIII antibodies from human serum has a minimal effect on virus neutralization, whereas neutralizing anti-EIII responses are more prominent in mouse serum (70, 71). The Western blotting and neutralization data obtained with our EIII chimeras are mostly in agreement with these observations, showing that these viruses may also be a useful tool to complement antibody depletion methods for discerning the role of EIII in immune responses. One interesting observation from the neutralization data was the relatively strong neutralization of the WNV/BAGV-EIII chimera (which showed NT_{50}s similar to those of WNV NY99 and WNV/KOUV-EIII with the anti-WNV MIAFs and NT_{50}s significantly higher than those of WNV/JEV-EIII and WNV/SLEV-EIII), despite having little antigenic cross-reactivity at the EIII level, as evidenced by the relative specificity of the anti-WNV EIII polyclonal antibody and the anti-BAGV MIAF. This may suggest that attachment to Vero cells and/or entry into Vero cells is less EIII dependent for the WNV/BAGV-EIII chimera than for the other viruses, with antibody recognition of other regions of E playing a more significant role in the neutralization of this virus than the neutralization of the others. Further studies would be necessary to confirm whether this is the case.

The *in vitro* growth, plaquing, and TS data suggest that substitution of EIII did not have a strong adverse effect on the chimeric viruses. The peak titers of all chimeras in Vero cells were within 10-fold of the titer of the parental wild-typeNY99 virus, which is a difference comparable to that previously reported for nonglycosylated variants of WNV NY99 (72). In addition, stability assays run with WNV NY99 gave results similar to those observed by Dowd et al. (2014), using reporter virus particles (73). Only the BAGV chimera had a >2-fold reduction in apparent half-life at 37°C, and the BAGV chimera was also the only virus to display any difference from wild-type virus NY99 in the TS comparison, having a reduced plaque size at 41°C compared to that at 37°C.

While the effects of chimerization were associated with some significant differences with respect to *in vitro* growth and plaquing phenotypes, they were even more pronounced *in vivo*, with differences in virulence between the EIII chimeras and WNV NY99 being observed after administration by the i.p. and/or i.c. route. Previous studies with engineered or selected mutants of WNV and some other JEV complex flaviviruses have identified single amino acid mutations that can attenuate mouse neuroinvasiveness (13, 15, 16, 74, 75) by multiple mechanisms that may be associated with direct or indirect effects on receptor binding or with increased glycosaminoglycan binding due to charge changes. Although it is possible that the reductions in the virulence of the EIII chimeras may have occurred due to negative effects on virion assembly, structure, or stability, the lack of obvious effects on *in vitro* behavior suggests that specific characteristics of the particular EIII sequence used likely play a more significant role in determining viral pathogenesis in mice. The range of infection outcomes and the changes in virus distribution in peripheral tissues following i.p. inoculation suggest that the introduction of alternative EIII sequences may have resulted in altered tissue tropisms for these viruses.

A very surprising observation was the strong attenuation of the virulence of the WNV/KOUV-EIII chimera. A recent study comparing the virulence of KOUV strain DaK Ar D 5443 and WNV NY99 in Swiss mice reported that KOUV was more virulent following peripheral inoculation than WNV NY99 and that the enhanced virulence appeared to be due to delayed innate and adaptive immune responses (76). Those authors hypothesized that this could be associated, at least in part, with a cluster of amino acid differences located within EIII (76). The chimeric WNV/KOUV-EIII showed a significant attenuation in virulence compared to the virulence of WNV NY99, with much lower mortality rates being detected following peripheral and intracranial inoculation, although some weight loss was observed for infected animals. In addition, the WNV/KOUV-EIII chimera showed significant differences in organ distribution from that of WNV NY99. This chimera produced a strong WNV NY99-like viremia and grew to titers equivalent to those of NY99 in the kidney, but there was minimal evidence for infection/replication in the other organs studied. Comparison of the KOUV EIII sequence with that of WNV NY99 (Fig. 1) revealed that the majority of the 11-amino-acid differences occur in regions of the protein that would be buried within the virion structure. However, a string of variable amino acids on the DE loop and a glutamic acid-to-aspartic acid substitution at residue 390 in a putative RGD/E integrin-binding motif would be surface accessible. None of these residues are in

immediate proximity to previously identified attenuating mutations in the BC loop (13), nor do they result in net charge changes typical of potentially attenuating glycosaminoglycan-binding adaptations. Nevertheless, our findings suggest that the reported increased virulence of wild-type KOUV in mouse models is not due to the amino acid differences that occur in EIII.

WNV/JEV-EIII behaved very similarly to WNV NY99 within the mouse model, showing virulence similar to that of NY99 following infection by both routes of administration. Both NY99 and WNV/JEV-EIII infection resulted in substantial temperature drops from day 8 until death, although, unlike WNV infections in humans and nonhuman primates, the infected mice showed no febrile phase (77, 78). In addition, mice infected with both viruses showed significant weight loss from day 7 onward. Subtle differences in organ distribution still occurred between WNV/JEV-EIII and NY99, not the least of which was a reduced frequency of neuroinvasion, despite similar overall mortality rates, with the titers of WNV/JEV-EIII in the other organs generally being lower than those of WNV NY99 in infected mice. In addition, WNV/JEV-EIII caused a protracted viremia, possibly suggesting less efficient clearance from the periphery by the immune system.

The virulence of WNV/SLEV-EIII was highly attenuated *in vivo*, even though it had *in vitro* growth, plaquing, stability, and TS phenotypes similar to those of WNV NY99. Even following i.c. inoculation, the virulence of WNV/SLEV-EIII appeared to be attenuated, with WNV/SLEV-EIII causing a significantly lower mortality rate than NY99 following a 10-PFU dose. After peripheral inoculation, the WNV/SLEV-EIII viremia was detectable but significantly lower than that of WNV NY99. In spite of the apparently rapid clearance of WNV/SLEV-EIII from the infected mice, the weight loss following infection in WNV/SLEV-EIII-infected mice was similar to that in WNV/KOUV-EIII-infected mice, raising the possibility that the virus may have infected and remained in an organ that was not examined.

In summary, these studies have demonstrated that viable flavivirus EIII chimeras that are structurally stable and replicate efficiently in mammalian and mosquito cell lines can be produced. These chimeras behaved significantly differently from one another and from the WNV NY99 backbone virus *in vivo*, with chimerization having substantial effects on virulence and the organ distribution. Although we have identified the differences in virus distribution at the organ level, more detailed studies are needed to determine whether specific cell types are differentially infected by wild-type WNV NY99 versus the EIII chimeras. Coupled with WNV mutants with other single- and multisite mutations, these chimeras may be used to more extensively define the contributions of EIII to the tropism and pathogenesis of WNV. This protein domain chimerization strategy is also applicable to investigations with other medically important flaviviruses.

ACKNOWLEDGMENTS

We thank B. Friedrich for help with the animal studies, as well as T. Wood and S. Widen at the Next Generation Sequencing core facility at UTMB. The studies made use of the facilities in the Galveston National Laboratory.

These studies were supported in part by start-up and pilot project funds provided to D.W.C.B. by the Institute for Human Infections and Immunity at UTMB. A.J.M. was supported by a James W. McLaughlin predoctoral fellowship and a Jeane B. Kempner predoctoral scholarship.

The funders had no role in study design, data collection and interpretation, or the decision to submit the work for publication.

FUNDING INFORMATION

This work, including the efforts of David Beasley, was funded by Institute for Human Infections and Immunity, UTMB.

Alexander McAuley was supported by a James W. McLaughlin predoctoral fellowship and a Jeane B. Kempner predoctoral scholarship.

REFERENCES

1. **Gould EA, Solomon T.** 2008. Pathogenic flaviviruses. Lancet **371:**500–509. http://dx.doi.org/10.1016/S0140-6736(08)60238-X.
2. **Kuhn RJ, Zhang W, Rossmann MG, Pletnev SV, Corver J, Lenches E, Jones CT, Mukhopadhyay S, Chipman PR, Strauss EG, Baker TS, Strauss JH.** 2002. Structure of dengue virus: implications for flavivirus organization, maturation, and fusion. Cell **108:**717–725. http://dx.doi.org/10.1016/S0092-8674(02)00660-8.
3. **Allison SL, Schalich J, Stiasny K, Mandl CW, Kunz C, Heinz FX.** 1995. Oligomeric rearrangement of tick-borne encephalitis virus envelope proteins induced by an acidic pH. J Virol **69:**695–700.
4. **Allison SL, Schalich J, Stiasny K, Mandl CW, Heinz FX.** 2001. Mutational evidence for an internal fusion peptide in flavivirus envelope protein E. J Virol **75:**4268–4275. http://dx.doi.org/10.1128/JVI.75.9.4268-4275.2001.
5. **Stiasny K, Allison SL, Schalich J, Heinz FX.** 2002. Membrane interactions of the tick-borne encephalitis virus fusion protein E at low pH. J Virol **76:**3784–3790. http://dx.doi.org/10.1128/JVI.76.8.3784-3790.2002.
6. **Chen Y, Maguire T, Marks RM.** 1996. Demonstration of binding of dengue virus envelope protein to target cells. J Virol **70:**8765–8772.
7. **Stiasny K, Allison SL, Marchler-Bauer A, Kunz C, Heinz FX.** 1996. Structural requirements for low-pH-induced rearrangements in the envelope glycoprotein of tick-borne encephalitis virus. J Virol **70:**8142–8147.
8. **Rey FA, Heinz FX, Mandl CW, Kunz C, Harrison SC.** 1995. The envelope glycoprotein from tick-borne encephalitis virus at 2 Å resolution. Nature **375:**291–298. http://dx.doi.org/10.1038/375291a0.
9. **Chu JJ-H, Rajamanonmani R, Li J, Bhuvanakantham R, Lescar J, Ng M-L.** 2005. Inhibition of West Nile virus entry by using a recombinant domain III from the envelope glycoprotein. J Gen Virol **86:**405–412. http://dx.doi.org/10.1099/vir.0.80411-0.
10. **Hung J-J, Hsieh M-T, Young M-J, Kao C-L, King C-C, Chang W.** 2004. An external loop region of domain III of dengue virus type 2 envelope protein is involved in serotype-specific binding to mosquito but not mammalian cells. J Virol **78:**378–388. http://dx.doi.org/10.1128/JVI.78.1.378-388.2004.
11. **Li C, Zhang L-Y, Sun M-X, Li P-P, Huang L, Wei J-C, Yao Y-L, Isahg H, Chen P-Y, Mao X.** 2012. Inhibition of Japanese encephalitis virus entry into the cells by the envelope glycoprotein domain III (EDIII) and the loop3 peptide derived from EDIII. Antiviral Res **94:**179–183. http://dx.doi.org/10.1016/j.antiviral.2012.03.002.
12. **Crill WD, Roehrig JT.** 2001. Monoclonal antibodies that bind to domain III of dengue virus E glycoprotein are the most efficient blockers of virus adsorption to Vero cells. J Virol **75:**7769–7773. http://dx.doi.org/10.1128/JVI.75.16.7769-7773.2001.
13. **Zhang S, Bovshik EI, Maillard R, Gromowski GD, Volk DE, Schein CH, Huang CYH, Gorenstein DG, Lee JC, Barrett ADT, Beasley DWC.** 2010. Role of BC loop residues in structure, function and antigenicity of the West Nile virus envelope protein receptor-binding domain III. Virology **403:**85–91. http://dx.doi.org/10.1016/j.virol.2010.03.038.
14. **Zhang S, Li L, Woodson SE, Huang CYH, Kinney RM, Barrett ADT, Beasley DWC.** 2006. A mutation in the envelope protein fusion loop attenuates mouse neuroinvasiveness of the NY99 strain of West Nile virus. Virology **353:**35–40. http://dx.doi.org/10.1016/j.virol.2006.05.025.
15. **Lee E, Hall RA, Lobigs M.** 2004. Common E protein determinants for attenuation of glycosaminoglycan-binding variants of Japanese encephalitis and West Nile viruses. J Virol **78:**8271–8280. http://dx.doi.org/10.1128/JVI.78.15.8271-8280.2004.
16. **Lee E, Lobigs M.** 2000. Substitutions at the putative receptor-binding site of an encephalitic flavivirus alter virulence and host cell tropism and reveal a role for glycosaminoglycans in entry. J Virol **74:**8867–8875. http://dx.doi.org/10.1128/JVI.74.19.8867-8875.2000.
17. **Roehrig JT, Butrapet S, Liss NM, Bennett SL, Luy BE, Childers T,**

Boroughs KL, Stovall JL, Calvert AE, Blair CD, Huang CYH. 2013. Mutation of the dengue virus type 2 envelope protein heparan sulfate binding sites or the domain III lateral ridge blocks replication in Vero cells prior to membrane fusion. Virology **441:**114–125. http://dx.doi.org/10.1016/j.virol.2013.03.011.

18. **Erb SM, Butrapet S, Moss KJ, Luy BE, Childers T, Calvert AE, Silengo SJ, Roehrig JT, Huang CYH, Blair CD.** 2010. Domain-III FG loop of the dengue virus type 2 envelope protein is important for infection of mammalian cells and Aedes aegypti mosquitoes. Virology **406:**328–335. http://dx.doi.org/10.1016/j.virol.2010.07.024.
19. **Huang Y-JS, Nuckols JT, Horne KM, Vanlandingham D, Lobigs M, Higgs S.** 2014. Mutagenesis analysis of T380R mutation in the envelope protein of yellow fever virus. Virol J **11:**60. http://dx.doi.org/10.1186/1743-422X-11-60.
20. **Elahi M, Islam MM, Noguchi K, Yohda M, Kuroda Y.** 2013. High resolution crystal structure of dengue-3 envelope protein domain III suggests possible molecular mechanisms for serospecific antibody recognition. Proteins **81:**1090–1095. http://dx.doi.org/10.1002/prot.24237.
21. **Volk DE, May FJ, Gandham SHA, Anderson A, von Lindern JJ, Beasley DWC, Barrett ADT, Gorenstein DG.** 2009. Structure of yellow fever virus envelope protein domain III. Virology **394:**12–18. http://dx.doi.org/10.1016/j.virol.2009.09.001.
22. **Gromowski GD, Barrett ND, Barrett ADT.** 2008. Characterization of dengue virus complex-specific neutralizing epitopes on envelope protein domain III of dengue 2 virus. J Virol **82:**8828–8837. http://dx.doi.org/10.1128/JVI.00606-08.
23. **Maillard RA, Jordan M, Beasley DWC, Barrett ADT, Lee JC.** 2008. Long range communication in the envelope protein domain III and its effect on the resistance of West Nile virus to antibody-mediated neutralization. J Biol Chem **283:**613–622. http://dx.doi.org/10.1074/jbc.M706031200.
24. **Gromowski GD, Barrett ADT.** 2007. Characterization of an antigenic site that contains a dominant, type-specific neutralization determinant on the envelope protein domain III (ED3) of dengue 2 virus. Virology **366:**349–360. http://dx.doi.org/10.1016/j.virol.2007.05.042.
25. **Volk DE, Chavez L, Beasley DWC, Barrett ADT, Holbrook MR, Gorenstein DG.** 2006. Structure of the envelope protein domain III of Omsk hemorrhagic fever virus. Virology **351:**188–195. http://dx.doi.org/10.1016/j.virol.2006.03.030.
26. **Yu S, Wuu A, Basu R, Holbrook MR, Barrett ADT, Lee JC.** 2004. Solution structure and structural dynamics of envelope protein domain III of mosquito- and tick-borne flaviviruses. Biochemistry **43:**9168–9176. http://dx.doi.org/10.1021/bi049324g.
27. **Li L, Barrett ADT, Beasley DWC.** 2005. Differential expression of domain III neutralizing epitopes on the envelope proteins of West Nile virus strains. Virology **335:**99–105. http://dx.doi.org/10.1016/j.virol.2005.02.011.
28. **Volk DE, Beasley DWC, Kallick DA, Holbrook MR, Barrett ADT, Gorenstein DG.** 2004. Solution structure and antibody binding studies of the envelope protein domain III from the New York strain of West Nile virus. J Biol Chem **279:**38755–38761. http://dx.doi.org/10.1074/jbc.M402385200.
29. **Bray M, Lai C-J.** 1991. Construction of intertypic chimeric dengue viruses by substitution of structural protein genes. Proc Natl Acad Sci U S A **88:**10342–10346. http://dx.doi.org/10.1073/pnas.88.22.10342.
30. **Pletnev AG, Bray M, Huggins J, Lai C-J.** 1992. Construction and characterization of chimeric tick-borne encephalitis/dengue type 4 viruses. Proc Natl Acad Sci U S A **89:**10532–10536. http://dx.doi.org/10.1073/pnas.89.21.10532.
31. **Chen W, Kawano H, Men R, Clark D, Lai C-J.** 1995. Construction of intertypic chimeric dengue viruses exhibiting type 3 antigenicity and neurovirulence for mice. J Virol **69:**5186–5190.
32. **Pletnev AG, Men R.** 1998. Attenuation of the Langat tick-borne flavivirus by chimerization with mosquito-borne flavivirus dengue type 4. Proc Natl Acad Sci U S A **95:**1746–1751. http://dx.doi.org/10.1073/pnas.95.4.1746.
33. **Chambers TJ, Nestorowicz A, Mason PW, Rice CM.** 1999. Yellow fever/Japanese encephalitis chimeric viruses: construction and biological properties. J Virol **73:**3095–3101.
34. **Monath TP, Soike K, Levenbook I, Zhang ZX, Arroyo J, Delagrave S, Myers G, Barrett AD, Shope RE, Ratterree M, Chambers TJ, Guirakhoo F.** 1999. Recombinant, chimaeric live, attenuated vaccine (ChimeriVax) incorporating the envelope genes of Japanese encephalitis (SA14-14-2) virus and the capsid and nonstructural genes of yellow fever (17D) virus is safe, immunogenic and protective in non-human primates. Vaccine **17:**1869–1882. http://dx.doi.org/10.1016/S0264-410X(98)00487-3.
35. **Huang CYH, Butrapet S, Pierro DJ, Chang G-JJ, Hunt AR, Bhamarapravati N, Gubler DJ, Kinney RM.** 2000. Chimeric dengue type 2 (vaccine strain PDK-53)/dengue type 1 virus as a potential candidate dengue type 1 virus vaccine. J Virol **74:**3020–3028. http://dx.doi.org/10.1128/JVI.74.7.3020-3028.2000.
36. **Caufour PS, Motta MC, Yamamura AM, Vazquez S, Ferreira II, Jabor AV, Bonaldo MC, Freire MS, Galler R.** 2001. Construction, characterization and immunogenicity of recombinant yellow fever 17D-dengue type 2 viruses. Virus Res **79:**1–14. http://dx.doi.org/10.1016/S0168-1702(01)00273-8.
37. **Pletnev AG, Putnak R, Speicher J, Wagar EJ, Vaughn DW.** 2002. West Nile virus/dengue type 4 virus chimeras that are reduced in neurovirulence and peripheral virulence without loss of immunogenicity or protective efficacy. Proc Natl Acad Sci U S A **99:**3036–3041. http://dx.doi.org/10.1073/pnas.022652799.
38. **Guirakhoo F, Pugachev K, Arroyo J, Miller C, Zhang ZX, Weltzin R, Georgakopoulos K, Catalan J, Ocran S, Draper K, Monath TP.** 2002. Viremia and immunogenicity in nonhuman primates of a tetravalent yellow fever-dengue chimeric vaccine: genetic reconstructions, dose adjustment, and antibody responses against wild-type dengue virus isolates. Virology **298:**146–159. http://dx.doi.org/10.1006/viro.2002.1462.
39. **Chambers TJ, Liang Y, Droll DA, Schlesinger JJ, Davidson AD, Wright PJ, Jiang X.** 2003. Yellow fever virus/dengue-2 virus and yellow fever virus/dengue-4 virus chimeras: biological characterization, immunogenicity, and protection against dengue encephalitis in the mouse model. J Virol **77:**3655–3668. http://dx.doi.org/10.1128/JVI.77.6.3655-3668.2003.
40. **Arroyo J, Miller CA, Catalan J, Monath TP.** 2001. Yellow fever vector live-virus vaccines: West Nile virus vaccine development. Trends Mol Med **7:**350–354. http://dx.doi.org/10.1016/S1471-4914(01)02048-2.
41. **Charlier N, Molenkamp R, Leyssen P, Paeshuyse J, Drosten C, Panning M, De Clercq E, Bredenbeek PJ, Neyts J.** 2004. Exchanging the yellow fever virus envelope proteins with Modoc virus prM and E proteins results in a chimeric virus that is neuroinvasive in SCID mice. J Virol **78:**7418–7426. http://dx.doi.org/10.1128/JVI.78.14.7418-7426.2004.
42. **Mathenge EGM, Parquet MDC, Funakoshi Y, Houhara S, Wong PF, Ichinose A, Hasebe F, Inoue S, Morita K.** 2004. Fusion PCR generated Japanese encephalitis virus/dengue 4 virus chimera exhibits lack of neuroinvasiveness, attenuated neurovirulence, and a dual-flavi immune response in mice. J Gen Virol **85:**2503–2513. http://dx.doi.org/10.1099/vir.0.80120-0.
43. **Pugachev KV, Guirakhoo F, Mitchell F, Ocran SW, Parsons M, Johnson BW, Kosoy OL, Lanciotti RS, Roehrig JT, Trent DW, Monath TP.** 2004. Construction of yellow fever/St. Louis encephalitis chimeric virus and the use of chimeras as a diagnostic tool. Am J Trop Med Hyg **71:**639–645.
44. **Huang CYH, Silengo SJ, Whiteman MC, Kinney RM.** 2005. Chimeric dengue 2 PDK-53/West Nile NY99 viruses retain the phenotypic attenuation markers of the candidate PDK-53 vaccine virus and protect mice against lethal challenge with West Nile virus. J Virol **79:**7300–7310. http://dx.doi.org/10.1128/JVI.79.12.7300-7310.2005.
45. **Chambers TJ, Jiang X, Droll DA, Liang Y, Wold WSM, Nickells J.** 2006. Chimeric Japanese encephalitis virus/dengue 2 virus infectious clone: biological properties, immunogenicity and protection against dengue encephalitis in mice. J Gen Virol **87:**3131–3140. http://dx.doi.org/10.1099/vir.0.81909-0.
46. **McGee CE, Tsetsarkin K, Vanlandingham DL, McElroy KL, Lang J, Guy B, Decelle T, Higgs S.** 2008. Substitution of wild-type yellow fever Asibi sequences for 17D vaccine sequences in ChimeriVax-dengue 4 does not enhance infection of Aedes aegypti mosquitoes. J Infect Dis **197:**686–692. http://dx.doi.org/10.1086/527328.
47. **Charlier N, Davidson AD, Dallmeier K, Molenkamp R, De Clercq E, Neyts J.** 2010. Replication of not-known-vector flaviviruses in mosquito cells is restricted by intracellular host factors rather than by the viral envelope proteins. J Gen Virol **91:**1693–1697. http://dx.doi.org/10.1099/vir.0.019851-0.
48. **Prow NA, May FJ, Westlake DJ, Hurrelbrink RJ, Biron RM, Leung JY, McMinn PC, Clark DC, Mackenzie JS, Lobigs M, Khromykh AA, Hall RA.** 2011. Determinants of attenuation in the envelope protein of the flavivirus Alfuy. J Gen Virol **92:**2286–2296. http://dx.doi.org/10.1099/vir.0.034793-0.
49. **Maharaj PD, Anishchenko M, Langevin SA, Fang Y, Reisen WK, Brault AC.** 2012. Structural gene (prME) chimeras of St Louis encephalitis virus

and West Nile virus exhibit altered in vitro cytopathic and growth phenotypes. J Gen Virol **93:**39–49. http://dx.doi.org/10.1099/vir.0.033159-0.
50. **Li X-F, Zhao W, Lin F, Ye Q, Wang H-J, Yang D, Li S-H, Zhao H, Xu Y-P, Ma J, Deng Y-Q, Zhang Y, Qin E-D, Qin C-F.** 2013. Development of chimaeric West Nile virus attenuated vaccine candidate based on the Japanese encephalitis vaccine strain SA14-14-2. J Gen Virol **94:**2700–2709. http://dx.doi.org/10.1099/vir.0.059436-0.
51. **Li X-F, Deng Y-Q, Yang H-Q, Zhao H, Jiang T, Yu X-D, Li S-H, Ye Q, Zhu S-Y, Wang H-J, Zhang Y, Ma J, Yu Y-X, Liu Z-Y, Li Y-H, Qin E-D, Shi P-Y, Qin C-F.** 2013. A chimeric dengue virus vaccine using Japanese encephalitis virus vaccine strain SA14-14-2 as backbone is immunogenic and protective against either parental virus in mice and nonhuman primates. J Virol **87:**13694–13705. http://dx.doi.org/10.1128/JVI.00931-13.
52. **Yoshii K, Sunden Y, Yokozawa K, Igarashi M, Kariwa H, Holbrook MR, Takashima I.** 2014. A critical determinant of neurological disease associated with highly pathogenic tick-borne flavivirus in mice. J Virol **88:**5406–5420. http://dx.doi.org/10.1128/JVI.00421-14.
53. **Wang H-J, Li X-F, Ye Q, Li S-H, Deng Y-Q, Zhao H, Xu Y-P, Ma J, Qin E-D, Qin C-F.** 2014. Recombinant chimeric Japanese encephalitis virus/tick-borne encephalitis virus is attenuated and protective in mice. Vaccine **32:**949–956. http://dx.doi.org/10.1016/j.vaccine.2013.12.050.
54. **Li Z, Yang H, Yang J, Lin H, Wang W, Liu L, Zhao Y, Liu L, Zeng X, Yu Y, Li Y.** 2014. Construction and preliminary investigation of a novel dengue serotype 4 chimeric virus using Japanese encephalitis vaccine strain SA14-14-2 as the backbone. Virus Res **191:**10–20. http://dx.doi.org/10.1016/j.virusres.2014.07.017.
55. **Saiyasombat R, Carrillo-Tripp J, Miller WA, Bredenbeek PJ, Blitvich BJ.** 2014. Substitution of the premembrane and envelope protein genes of Modoc virus with the homologous sequences of West Nile virus generates a chimeric virus that replicates in vertebrate but not mosquito cells. Virol J **11:**150. http://dx.doi.org/10.1186/1743-422X-11-150.
56. **Gromowski GD, Firestone C-Y, Hanson CT, Whitehead SS.** 2014. Japanese encephalitis virus vaccine candidates generated by chimerization with dengue virus type 4. Vaccine **32:**3010–3018. http://dx.doi.org/10.1016/j.vaccine.2014.03.062.
57. **Kinney RM, Huang CYH, Whiteman MC, Bowen RA, Langevin SA, Miller BR, Brault AC.** 2006. Avian virulence and thermostable replication of the North American strain of West Nile virus. J Gen Virol **87:**3611–3622. http://dx.doi.org/10.1099/vir.0.82299-0.
58. **Beasley DWC, Whiteman MC, Zhang S, Huang CYH, Schneider BS, Smith DR, Gromowski GD, Higgs S, Kinney RM, Barrett ADT.** 2005. Envelope protein glycosylation status influences mouse neuroinvasion phenotype of genetic lineage 1 West Nile virus strains. J Virol **79:**8339–8347. http://dx.doi.org/10.1128/JVI.79.13.8339-8347.2005.
59. **Ergunay K, Bakonyi T, Nowotny N, Ozkul A.** 2015. Close relationship between West Nile virus from Turkey and lineage 1 strain from Central African Republic. Emerg Infect Dis **21:**352–355. http://dx.doi.org/10.3201/eid2102.141135.
60. **Worwa G, Wheeler SS, Brault AC, Reisen WK.** 2015. Comparing competitive fitness of West Nile virus strains in avian and mosquito hosts. PLoS One **10:**e0125668. http://dx.doi.org/10.1371/journal.pone.0125668.
61. **May FJ, Li L, Davis CT, Galbraith SE, Barrett ADT.** 2010. Multiple pathways to the attenuation of West Nile virus in south-east Texas in 2003. Virology **405:**8–14. http://dx.doi.org/10.1016/j.virol.2010.04.022.
62. **Jia Y, Moudy RM, Dupuis AP, Ngo KA, Maffei JG, Jerzak GVS, Franke MA, Kauffman EB, Kramer LD.** 2007. Characterization of a small plaque variant of West Nile virus isolated in New York in 2000. Virology **367:**339–347. http://dx.doi.org/10.1016/j.virol.2007.06.008.
63. **Beasley DWC, Holbrook MR, Travassos Da Rosa APA, Coffey L, Carrara A-S, Phillippi-Falkenstein K, Bohm RP, Ratterree MS, Lillibridge KM, Ludwig GV, Estrada-Franco J, Weaver SC, Tesh RB, Shope RE, Barrett ADT.** 2004. Use of a recombinant envelope protein subunit antigen for specific serological diagnosis of West Nile virus infection. J Clin Microbiol **42:**2759–2765. http://dx.doi.org/10.1128/JCM.42.6.2759-2765.2004.
64. **Reagan RL, Schenck DM, Harmon MP, Brueckner AL.** 1952. Effect of West Nile virus in the Swiss albino mouse and the cave bat. J Bacteriol **64:**79–81.
65. **Peña J, Plante JA, Carillo AC, Roberts KK, Smith JK, Juelich TL, Beasley DWC, Freiberg AN, Labute MX, Naraghi-Arani P.** 2014. Multiplexed digital mRNA profiling of the inflammatory response in the West Nile Swiss Webster mouse model. PLoS Negl Trop Dis **8:**e3216. http://dx.doi.org/10.1371/journal.pntd.0003216.
66. **Cruz-Oliveira C, Freire JM, Conceição TM, Higa LM, Castanho MARB, Da Poian AT.** 2015. Receptors and routes of dengue virus entry into the host cells. FEMS Microbiol Rev **39:**155–170. http://dx.doi.org/10.1093/femsre/fuu004.
67. **Nybakken GE, Oliphant T, Johnson S, Burke S, Diamond MS, Fremont DH.** 2005. Structural basis of West Nile virus neutralization by a therapeutic antibody. Nature **437:**764–769. http://dx.doi.org/10.1038/nature03956.
68. **Bielefeldt-Ohmann H, Beasley DW, Fitzpatrick DR, Aaskov JG.** 1997. Analysis of a recombinant dengue-2 virus-dengue-3 virus hybrid envelope protein expressed in a secretory baculovirus system. J Gen Virol **78:**2723–2733. http://dx.doi.org/10.1099/0022-1317-78-11-2723.
69. **Gallichotte EN, Widman DG, Yount BL, Wahala WM, Durbin A, Whitehead S, Sariol CA, Crowe JE, de Silva AM, Baric RS.** 2015. A new quaternary structure epitope on dengue virus serotype 2 is the target of durable type-specific neutralizing antibodies. mBio **6:**e01461-15. http://dx.doi.org/10.1128/mBio.01461-15.
70. **Wahala WMPB, Kraus AA, Haymore LB, Accavitti-Loper MA, de Silva AM.** 2009. Dengue virus neutralization by human immune sera: role of envelope protein domain III-reactive antibody. Virology **392:**103–113. http://dx.doi.org/10.1016/j.virol.2009.06.037.
71. **Dowd KA, Pierson TC.** 2011. Antibody-mediated neutralization of flaviviruses: a reductionist view. Virology **411:**306–315. http://dx.doi.org/10.1016/j.virol.2010.12.020.
72. **Shirato K, Miyoshi H, Goto A, Ako Y, Ueki T, Kariwa H, Takashima I.** 2004. Viral envelope protein glycosylation is a molecular determinant of the neuroinvasiveness of the New York strain of West Nile virus. J Gen Virol **85:**3637–3645. http://dx.doi.org/10.1099/vir.0.80247-0.
73. **Dowd KA, Mukherjee S, Kuhn RJ, Pierson TC.** 2014. Combined effects of the structural heterogeneity and dynamics of flaviviruses on antibody recognition. J Virol **88:**11726–11737. http://dx.doi.org/10.1128/JVI.01140-14.
74. **Hurrelbrink RJ, McMinn PC.** 2001. Attenuation of Murray Valley encephalitis virus by site-directed mutagenesis of the hinge and putative receptor-binding regions of the envelope protein. J Virol **75:**7692–7702. http://dx.doi.org/10.1128/JVI.75.16.7692-7702.2001.
75. **Lee E, Lobigs M.** 2008. E protein domain III determinants of yellow fever virus 17D vaccine strain enhance binding to glycosaminoglycans, impede virus spread, and attenuate virulence. J Virol **82:**6024–6033. http://dx.doi.org/10.1128/JVI.02509-07.
76. **Prow NA, Setoh YX, Biron RM, Sester DP, Kim KS, Hobson-Peters J, Hall RA, Bielefeldt-Ohmann H.** 2014. The West Nile virus-like flavivirus Koutango is highly virulent in mice due to delayed viral clearance and the induction of a poor neutralizing antibody response. J Virol **88:**9947–9962. http://dx.doi.org/10.1128/JVI.01304-14.
77. **Melnick JL, Paul JR, Riordan JT, Barnett VH, Goldblum N, Zabin E.** 1951. Isolation from human sera in Egypt of a virus apparently identical to West Nile virus. Proc Soc Exp Biol Med **77:**661–665. http://dx.doi.org/10.3181/00379727-77-18884.
78. **Weiss D, Carr D, Kellachan J, Tan C, Phillips M, Bresnitz E, Layton M.** 2001. Clinical findings of West Nile virus infection in hospitalized patients, New York and New Jersey, 2000. Emerg Infect Dis **7:**654–658. http://dx.doi.org/10.3201/eid0704.017409.